EURASIP Journal on Wireless Communications and Networking 2004:1, 172–183

Coding Across Multicodes and Time in CDMA Systems Employing MMSE Multiuser Detector

Jeongsoon Park
School of Electrical and Computer Engineering, Purdue University, West Lafayette, IN 47907, USA
Email: jspark@purdue.edu

Jong-Han Lim
Samsung Electronics, 416 Maetan 3-dong, Paldal-gu, Suwon-si, South Korea 442-742
Email: jonghan.lim@samsung.com

Saul B. Gelfand
School of Electrical and Computer Engineering, Purdue University, West Lafayette, IN 47907, USA
Email: gelfand@ecn.purdue.edu

Received 1 November 2003; Revised 23 March 2004

When combining a multicode CDMA system with convolutional coding, two methods have been considered in the literature. In one method, coding is across time in each multicode channel while in the other the coding is across both multicodes and time. In this paper, a performance/complexity analysis of decoding metrics and trellis structures for the two schemes is carried out. It is shown that the latter scheme can exploit the multicode diversity inherent in convolutionally coded direct sequence code division multiple access (DS-CDMA) systems which employ minimum mean squared error (MMSE) multiuser detectors. In particular, when the MMSE detector provides sufficiently different signal-to-interference ratios (SIRs) for the multicode channels, coding across multicodes and time can obtain significant performance gain over coding across time, with nearly the same decoding complexity.

Keywords and phrases: multicode CDMA, MMSE detector, multicode diversity.

1. INTRODUCTION

In third generation code division multiple access (CDMA) systems, multimedia data transmission needs to support variable data rates. Multicode CDMA is one method to do this, the basic idea of which is to allocate more spreading codes to users with higher data rates [1].

There are two methods which have been suggested to combine a multicode CDMA system with convolutional coding. In one approach, a serial-to-parallel (S/P) conversion precedes the convolutional coding [2], while in the other approach the S/P conversion follows the convolutional coding [3]. When S/P conversion precedes convolutional coding, the coding is only across time in each multicode channel, while when the order is reversed, the coding is across both multicodes and time.The latter approach has also been applied to multicarrier CDMA systems [4] and multiantenna CDMA systems [5]. These systems assume that the temporal diversity associated with convolutional coding is fully exploited by interleaving. The case where the fading is slow and the delay constraints do not allow the adoption of an interleaver is considered in [5], where instead spatial diversity for the coded symbols is provided by the transmit antenna. None of these methods employ multiuser detection, which may be additionally required to get the desired performance.

To suppress interference among users in a multiuser environment, a minimum mean squared error (MMSE) multiuser detector is often employed [6] and can be combined with convolutional coding to further improve performance [7]. In this paper, we consider a multicode CDMA system with convolutional coding and an MMSE detector. As in [5] (which does not employ multiuser detection), we focus on the situation where temporal diversity is not available, that is, the fading is too slow to employ an interleaver. Unless the crosscorrelations between all the users' spreading codes are equal, the signal-to-interference ratios (SIRs) for the users at the MMSE detector output are different. When only coding across time (CT) is employed and one of the multicodes of the desired user has significantly lower SIR at the MMSE detector output, it is shown that the average coded performance

over all multicodes is dominated by the worst multicode SIR. However, when coding across multicodes and time (CMT) is used, each convolutionally coded symbol is transmitted over several multicodes with different SIRs, and it is shown that the average coded performance over all the multicodes is related to the average multicode SIR. Thus, the diversity inherent in multicodes at the MMSE multiuser detector output can be exploited with CMT.

We develop and analyze maximum-likelihood (ML) decoding for both CMT and CT in multicode CDMA systems. For CMT, the optimal decoding metric is rather complex. To reduce the complexity, three suboptimal decoding metrics are also considered, including one which has the same complexity as CT (we call this latter metric the "conventional" one in that it ignores the correlation due to multicoding and decodes the convolutional coding in a conventional way). In CMT, for metrics other than the conventional one, there exist both time-invariant and time-varying trellis representations. The time-invariant trellis is useful for analysis, while the time-varying trellises can significantly reduce the decoding complexity depending upon the number of multicodes and the code rate.

To find a true upper bound on the user bit error rate (BER) for the ML and suboptimal decoding, the Laplace transform method can be combined with the transfer function method [8]. But using the residue method for the evaluation of the Laplace integral results in computationally complex symbolic operation to evaluate the transfer function. However, if the Gauss-Chebyshev quadrature rule is used for numerical integration, each pairwise error probability (PEP) can be expressed in a product form and the transfer function method can be applied. This is the approach taken in this paper.

The paper is organized as follows. In Section 2, the system model is presented. In Section 3, decoding metrics and trellises for CMT are proposed, and in Section 4 a theoretical upper bound on BER for each metric is derived. Simulation results are provided in Section 5 and some conclusions and future work are discussed in Section 6.

2. SYSTEM MODELS

The transmitter block diagram of a multicode CDMA system with CT and CMT for desired user k is shown in Figure 1, and the corresponding receiver block diagrams are shown in Figure 2. The mth information bit for user k is $d_k[m]$. Let $1/T_k$ denote the information bit rate, m_k the number of multicodes, and R_k the code rate, for user k. The ith coded bit of multicode j for user k is $c_{k,j}[i] \in \{0,1\}$, and the corresponding binary code symbol is $b_{k,j}[i] = 2c_{k,j}[i] - 1 \in \{+1,-1\}$.

The code symbol rate for each multicode channel of user k is $1/m_k T_k R_k$. For the purpose of designing and implementing the MMSE multiuser detector, it is simplest to require that these code symbol rates are the same for all users, that is, $1/m_k T_k R_k = 1/T$ for some T. A special case of this occurs when the user information bit rates are all integral multiples of the lowest bit rate $1/T_b = 1/\max_k T_k$, and the multicodes are assigned such that $m_k = T_b/T_k$ and all users employ the same rate $1/n$ convolutional code (CC). For ease of presentation we will assume this case in the sequel. (A more general but similarly treated situation is the case when $m_k \neq T_b/T_k$ for some users $k \in A$ and all other users are assigned $m_j = T_b/T_j$ multicodes for $j \notin A$. Each user $j \notin A$ employs the same rate $1/n$ CC. The code rate R_k, $k \in A$, becomes $T_b/T_k m_k n$ and the integer $m_k \geq 1$ must satisfy $m_k > T_b/T_k n$ to make $T_b/T_k m_k n$ a realizable CC rate which should be less than 1.) Note that the processing gains of CT and CMT are equal when the chip rates of the spreading waveforms of the two systems are equal. However, the encoder and decoder of CMT requires m_k times faster processing speed at both the encoder and decoder than CT.

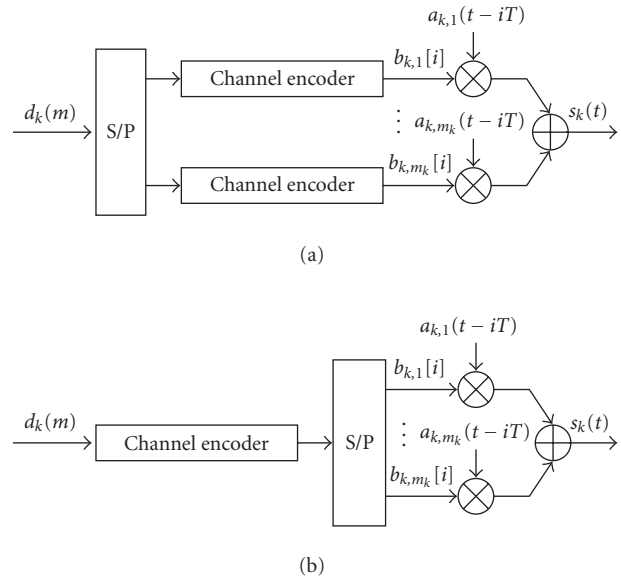

FIGURE 1: Transmitter of desired user k. (a) Coding across time, (b) coding across multicodes and time.

In CDMA systems, the transmitted signal for user k is

$$s_k(t) = \sum_{j=1}^{m_k} \sum_{i=-\infty}^{i=\infty} A_{k,j} b_{k,j}[i] a_{k,j}(t - iT), \tag{1}$$

where $A_{k,j}$ is the received signal amplitude of the jth multicode of the kth user, and $a_{k,j}(t)$ is the normalized spreading waveform of the jth multicode of the kth user with support in $[0,T]$. The spreading waveform $a_{k,j}(t)$ is

$$a_{k,j}(t) = \sum_{m=0}^{N-1} p_{k,j}[m] \psi(t - mT_c), \tag{2}$$

where $p_{k,j}[m] \in \{+1/\sqrt{N}, -1/\sqrt{N}\}$, $m = 0,\ldots,N-1$, is the spreading sequence, N is the processing gain, and $\psi(t)$ is

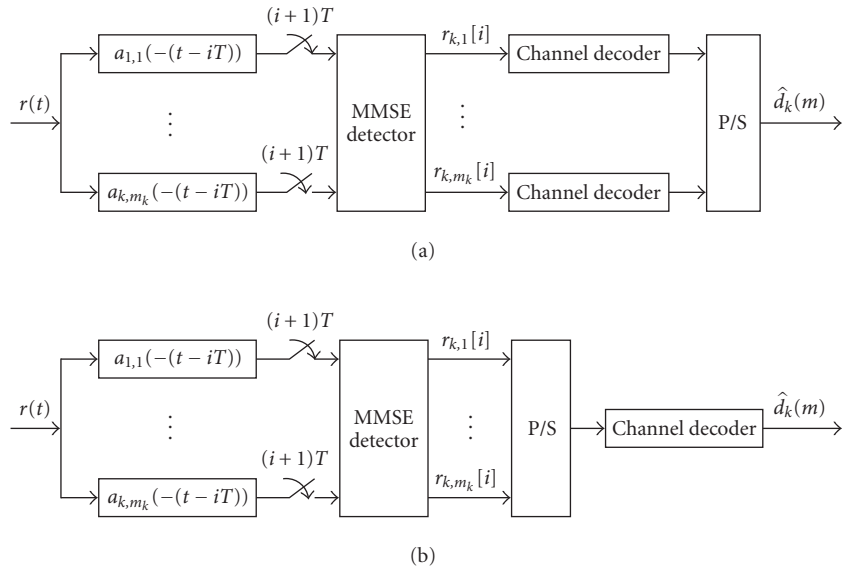

FIGURE 2: Receiver of desired user k. (a) Coding across time, (b) coding across multicodes and time.

the normalized rectangular chip waveform with support in $[0, T_c]$, $\int_0^{T_c} \psi^2(t)dt = 1$.

The received signal in a downlink CDMA additive white Gaussian noise (AWGN) channel is

$$r(t) = \sum_{k=1}^{K} s_k(t) + n(t), \tag{3}$$

where $n(t)$ is (real) white Gaussian noise with power spectral density σ^2, and K is the number of active users. The matched filter output of multicode j of user k in the ith code symbol interval is

$$y_{k,j}[i] = \int_{iT}^{(i+1)T} a_{k,j}(t - iT)r(t)dt. \tag{4}$$

The vector $\mathbf{y}_i = [y_{1,1}[i], \ldots, y_{1,m_1}[i], y_{2,1}[i], \ldots, y_{K,m_K}[i]]^T$ is given by [6]

$$\mathbf{y}_i = \mathbf{RAb}_i + \mathbf{n}_i, \tag{5}$$

where $\mathbf{R}$ is the crosscorrelation matrix

$$(\mathbf{R})_{\sum_{p=1}^{k-1} m_p + j, \sum_{p=1}^{l-1} m_p + m} = \int_0^T a_{k,j}(t)a_{l,m}(t)dt, \tag{6}$$

$\mathbf{A} = \text{diag}\{A_{1,1}, \ldots, A_{1,m_1}, A_{2,1}, \ldots, A_{K,m_K}\}$, and $\mathbf{b}_i = [b_{1,1}[i], \ldots, b_{1,m_1}[i], b_{2,1}[i], \ldots, b_{K,m_K}[i]]^T$. The covariance matrix of the Gaussian noise vector $\mathbf{n}_i = [n_{1,1}[i], \ldots, n_{1,m_1}[i], n_{2,1}[i], \ldots, n_{K,m_K}[i]]^T$ is $\sigma^2\mathbf{R}$ and $\{\mathbf{n}_i\}$ is i.i.d.

Since we do not employ an interleaver in our system, $\{\mathbf{b}_i\}$ is a correlated sequence due to the convolutional coding. Furthermore, for CMT (but not CT) the components of $\mathbf{b}_i$ associated with the same user but different multicodes are correlated for the same reason. However, the correlation between code symbols becomes smaller as the constraint length gets larger. We will assume that $b_{k,j}[i]$ and $b_{k,j'}[i']$ are independent for $i \neq i'$ or $j \neq j'$. Our simulations show this to be a good approximation with rate 1/2 or 1/3 codes and constraint length greater than or equal to 5. This approximation is employed in the design of the MMSE detector below, and to design and analyze the decoding metrics in Sections 3 and 4.

The MMSE detector output for multicode j of desired user k in the ith symbol interval is $r_{k,j}[i] = \boldsymbol{\omega}_{k,j}^T \mathbf{y}_i$, where [6]

$$\boldsymbol{\omega}_{k,j} = \left(\mathbf{R} + \sigma^2\mathbf{A}^{-2}\right)^{-1}\mathbf{e}_{k,j}, \tag{7}$$

and $\mathbf{e}_{k,j}$ is the vector whose elements are all zeros except for the $(\sum_{p=1}^{k-1} m_p + j)$th element which is 1. Thus the MMSE detector for all $\sum_{p=1}^{K} m_p$ multicodes can be expressed as

$$\mathbf{M} = [\boldsymbol{\omega}_{1,1}, \ldots, \boldsymbol{\omega}_{k,m_k}, \ldots, \boldsymbol{\omega}_{K,m_K}] = \left(\mathbf{R} + \sigma^2\mathbf{A}^{-2}\right)^{-1}. \tag{8}$$

3. DECODING METRICS AND TRELLISES

For both CT and CMT, the decoder input of desired user k is given by $\{(\mathbf{r}_i^k)^T\}_{i=-\infty}^{\infty}$, where $\mathbf{r}_i^k = [r_{k,1}[i], r_{k,2}[i], \ldots, r_{k,m_k}[i]]^T$. However, for CT m_k decoders are required and the input of each decoder with index $j = 1, \ldots, m_k$ is $\{\ldots, r_{k,j}[i], r_{k,j}[i+1], \ldots\}$, while for CMT one decoder is needed and the input to the decoder is $\{\ldots, r_{k,1}[i],$

$r_{k,2}[i],\ldots,r_{k,m_k}[i],r_{k,1}[i+1],\ldots\}$. $\mathbf{r}_i^k$ can be expressed as

$$\mathbf{r}_i^k = (\hat{\mathbf{R}}^k \odot \mathbf{I}_k)\mathbf{A}^k\mathbf{b}_i^k + \mathbf{i}_i^k + \bar{\mathbf{i}}_i^k + \hat{\mathbf{n}}_i^k, \tag{9}$$

where

$$\begin{aligned}
(\hat{\mathbf{R}}^k)_{j,l} &= (\boldsymbol{\omega}_{k,j}^T\mathbf{R})_{\sum_{p=1}^{k-1}m_p+l}, \quad j=1,\ldots,m_k,\ l=1,\ldots,m_k,\\
\mathbf{A}^k &= \operatorname{diag}\{A_{k,1}\ldots,A_{k,m_k}\},\\
\mathbf{b}_i^k &= [b_{k,1}[i],\ldots,b_{k,m_k}[i]]^T,\\
\mathbf{i}_i^k &= (\hat{\mathbf{R}}^k - (\hat{\mathbf{R}}^k \odot \mathbf{I}_k))\mathbf{A}^k\mathbf{b}_i^k,\\
\bar{\mathbf{i}}_i^k &= \bar{\tilde{\mathbf{R}}}^k\bar{\mathbf{A}}^k\bar{\mathbf{b}}_i^k,\\
\left(\bar{\tilde{\mathbf{R}}}^k\right)_{j,l} &= \begin{cases}(\boldsymbol{\omega}_{k,j}\mathbf{R})_l, & j=1,\ldots,m_k,\\ & l=1,\ldots,\sum_{p=1}^{k-1}m_p,\\ (\boldsymbol{\omega}_{k,j}\mathbf{R})_{l+m_k}, & j=1,\ldots,m_k,\\ & l=\sum_{p=1}^{k-1}m_p+1,\ldots,\sum_{\substack{p=1\\p\neq k}}^{K}m_p,\end{cases}\\
\bar{\mathbf{A}}^k &= \operatorname{diag}\{A_{1,1},\ldots,A_{k-1,m_{k-1}},A_{k+1,1},\ldots,A_{K,m_K}\},\\
\bar{\mathbf{b}}_i^k &= [b_{1,1}[i],\ldots,b_{k-1,m_{k-1}}[i],b_{k+1,1}[i],\ldots,b_{K,m_K}[i]]^T,\\
\hat{\mathbf{n}}_i^k &= [\boldsymbol{\omega}_{k,1}^T\mathbf{n}_i,\ldots,\boldsymbol{\omega}_{k,m_k}^T\mathbf{n}_i]^T,
\end{aligned} \tag{10}$$

$\mathbf{I}_k$ is $m_k \times m_k$ identity matrix and $\odot$ represents elementwise product of two matrices. The covariance matrix of $\hat{\mathbf{n}}_i^k$ is $\sigma^2\bar{\mathbf{R}}^k$ where $(\bar{\mathbf{R}}^k)_{j,l} = \boldsymbol{\omega}_{k,j}^T\mathbf{R}\boldsymbol{\omega}_{k,l}$, $j=1,\ldots,m_k$, $l=1,\ldots,m_k$.

In CT, the kth user employs m_k encoders and the trellis stage index t^j for jth encoder is related to the input bit index m by $t^j(m) = \lfloor (m-1)/m_k \rfloor + 1$ and $m(t^j) = (t^j-1)m_k + j$, $j=1,\ldots,m_k$. Assuming $\mathbf{i}_i^k$ and $\bar{\mathbf{i}}_i^k$ are well approximated as Gaussian [6], the branch metric corresponding to the t^jth transition reduces to

$$\mu_{t^j}^k = \sum_{l=1}^{n}\left(r_{k,j}[(t^j-1)n+l] - (\hat{\mathbf{R}}^k)_{j,j}A_{k,j}b_{k,j}[(t^j-1)n+l]\right)^2. \tag{11}$$

In CMT, m_k code symbols are aligned at the same symbol interval and their MMSE detector outputs are correlated with each other. The covariance matrix $\bar{\boldsymbol{\Phi}}^k$ of $\bar{\mathbf{i}}_i^k$ is given by $\bar{\boldsymbol{\Phi}}^k = \bar{\tilde{\mathbf{R}}}^k\bar{\mathbf{A}}^k(\bar{\mathbf{A}}^k)^T(\bar{\tilde{\mathbf{R}}}^k)^T$ and that of $\hat{\mathbf{n}}_i^k$ is $\sigma^2\bar{\mathbf{R}}^k$. Assuming $\bar{\mathbf{i}}_i^k$ is well-approximated as Gaussian, the branch metric corresponding to the tth transition is given by

$$\mu_t^{k,1} = \sum_{i=\underline{i}_t}^{\bar{i}_t}\left(\mathbf{r}_i^k - \hat{\mathbf{R}}^k\mathbf{A}^k\mathbf{b}_i^k\right)^T\left(\sigma^2\bar{\mathbf{R}}^k + \bar{\boldsymbol{\Phi}}^k\right)^{-1}\left(\mathbf{r}_i^k - \hat{\mathbf{R}}^k\mathbf{A}^k\mathbf{b}_i\right), \tag{12}$$

where $\underline{i}_t$ and $\bar{i}_t$ depend on the choice of decoding trellis discussed in the sequel.

To reduce the complexity, suboptimal metrics are considered. If the Viterbi decoder does not consider $\mathbf{i}_i^k$, the corresponding suboptimal metric is given by

$$\begin{aligned}\mu_t^{k,2} = \sum_{i=\underline{i}_t}^{\bar{i}_t}&\left(\mathbf{r}_i^k - (\hat{\mathbf{R}}^k \odot \mathbf{I}_k)\mathbf{A}^k\mathbf{b}_i^k\right)^T\left(\sigma^2\bar{\mathbf{R}}^k + \bar{\boldsymbol{\Phi}}^k\right)^{-1}\\ &\times\left(\mathbf{r}_i^k - (\hat{\mathbf{R}}^k \odot \mathbf{I}_k)\mathbf{A}^k\mathbf{b}_i^k\right).\end{aligned} \tag{13}$$

If the decoder ignores the correlation of $\bar{\mathbf{i}}_i^k$ and $\hat{\mathbf{n}}_i$, the corresponding suboptimal metric is given by

$$\mu_t^{k,3} = \sum_{i=\underline{i}_t}^{\bar{i}_t}\left(\mathbf{r}_i^k - \hat{\mathbf{R}}^k\mathbf{A}^k\mathbf{b}_i^k\right)^T\left(\mathbf{r}_i^k - \hat{\mathbf{R}}^k\mathbf{A}^k\mathbf{b}_i^k\right). \tag{14}$$

Finally, the suboptimal metric

$$\mu_t^{k,4} = \sum_{i=\underline{i}_t}^{\bar{i}_t}\left(\mathbf{r}_i^k - (\hat{\mathbf{R}}^k \odot \mathbf{I}_k)\mathbf{A}^k\mathbf{b}_i^k\right)^T\left(\mathbf{r}_i^k - (\hat{\mathbf{R}}^k \odot \mathbf{I}_k)\mathbf{A}^k\mathbf{b}_i^k\right) \tag{15}$$

corresponds to both of the above simplifications and is just the conventional decoding metric for vector observations in additive white Gaussian multiple access interference and (independent) AWGN.

We first consider the time-invariant trellis for CMT. In the time-invariant trellis, one transition corresponds to $\tilde{m} = \mathrm{LCM}(n,m_k)/n$ transitions in the code trellis and any combination of m_k and n can be treated. For the time-invariant trellis we have $\underline{i}_t = \tilde{i}(t-1)+1$ and $\bar{i}_t = \tilde{i}t$, where $\tilde{i} = \mathrm{LCM}(n,m_k)/m_k$ in the branch metrics above. The case where n is divisible by m_k corresponds to a special case of this time-invariant trellis with $\tilde{m}=1$, $\tilde{i} = n/m_k$. Here a transition occurs at each information bit input and the state transitions are equivalent to those of the CC. In this case we say that m_k *and* n *are matched*. If we define the decoding complexity as the number of visited branches per decoded bit, the decoding complexity of the CC is $2^{\nu+1}$, where ν is the memory of the CC. The decoding complexity of the time-invariant trellis is that of the CC multiplied by $2^{\tilde{m}-1}/\tilde{m}$, when we employ metrics other than that in (15) (if the conventional metric (15) is used, the decoding complexity is equal to that of the CC regardless of $\tilde{m}$).

Mismatched cases of m_k and n can be dealt with using the time-invariant-trellis approach. But with a time-invariant trellis we have to search over $2^{\tilde{m}}$ branches at each state for each transition, and for some m_k and n this complexity can be prohibitive. However, if we design the trellis so that a transition occurs for information input bits corresponding to an appropriate number of observation vectors of the decoder depending on m_k and n, it turns out that the decoding complexity can be significantly reduced. But because of the mismatch of m_k and n, the trellis becomes time varying.

To describe time-varying trellises for CMT, we first define the maximum number of information bit inputs $\bar{m}$ to generate all of the m_k code symbols which cause multicode

interference with each other at each CC state transition. When m_k and n are matched, $\tilde{m} = 1$ which reduces to the case of CC. When $m_k < n$ and n is not divisible by m_k, $\tilde{m} = 2$ because multicode interference can affect code symbols corresponding to two transitions in the code trellis. When $m_k > n$ and $(m_k - n\lfloor m_k/n \rfloor) = \mathrm{GCD}(n, m_k)$, $\tilde{m} = \lfloor m_k/n \rfloor + \mathbf{1}_{\{(m_k - n\lfloor m_k/n \rfloor) \geq 1\}}$. When $m_k > n$ and $(m_k - n\lfloor m_k/n \rfloor) \neq \mathrm{GCD}(n, m_k)$, $\tilde{m} = \lfloor m_k/n \rfloor + \mathbf{1}_{\{(m_k - n\lfloor m_k/n \rfloor) \geq 1\}} + \mathbf{1}_{\{(m_k - n\lfloor m_k/n \rfloor) \geq 2\}}$. In the following time-varying trellis discussion, we are interested in mismatch of m_k and n, that is, when $\tilde{m} \geq 2$, and we consider both fixed and variable state augmentation approaches corresponding to whether the CMT trellis obtained by augmenting the input bits and/or state in the CC trellis varies from one transition to another (in addition to the number and/or structure of the CMT branch metrics).

We first consider fixed state augmentation time-varying trellises.

(i) When $m_k < n$ and n is not divisible by m_k, the CC state is augmented by 1 bit, but the number of information input bits per transition is kept equal to one. For this fixed state augmentation time-varying trellis, $\bar{i}_t = \max_i(im_k \leq tn)$ and $\underline{i}_t = \bar{i}(t-1) + 1$ in the branch metrics in (12), (13), (14), and (15). The computational complexity of the fixed state augmentation time-varying trellis decoding is that of the CC multiplied by 2^1. If n is divisible by m_k then the CMT trellis is just the CC trellis.

(ii) When $m_k > n$, for some transitions more than one input bit is required and there is no simple fixed state augmentation time-varying trellis. It is possible to modify the variable state augmentation time-varying trellis, below to enforce a fixed state augmentation, but such an approach has no advantage either intuitively or computationally so we do not elaborate on it here.

Next we consider variable state augmentation time-varying trellises:

(i) When $m_k < n$ and n is not divisible by m_k, at the tth transition, if $(t-1)n$ is not divisible by m_k, the CC state is augmented by 1 bit and otherwise it is not augmented. The number of information input bits at the tth transition is one if $(t-1)n$ is not divisible by m_k and is two otherwise. For this variable state augmentation time-varying trellis, $\bar{i}_t = \lfloor (x_t + 1)n/m_k \rfloor$ and $\underline{i}_t = (x_t - 1)n/m_k + 1$ when $(t-1)$ is divisible by $(\tilde{m} - 1)$ and otherwise $\bar{i}_t = \lfloor y_t n/m_k \rfloor$ and $\underline{i}_t = \lfloor (y_t - 1)n/m_k \rfloor + 1$, where $x_t = (t-1)/(\tilde{m}-1) \cdot \tilde{m} + 1$ and $y_t = t + \lfloor (t-1)/(\tilde{m}-1) \rfloor + 1$ in the branch metrics in (12), (13), (14), and (15). The computational complexity of the variable state augmentation time-varying trellis decoding is that of the CC multiplied by $2 \cdot (\tilde{m} - 1)/\tilde{m}$, which is always less than the factor of 2 for the fixed state augmentation time-varying trellis decoding. When $\tilde{m} = 2$, the variable state augmentation time-varying trellis reduces to a time-invariant trellis with the same decoding complexity as CC. If n is divisible by m_k, then the CMT trellis is just the CC trellis.

(ii) When $m_k > n$ and m_k is not divisible by n, at the tth transition, if $(t-1)m_k$ is not divisible by n, the CC state is augmented by 1 bit and otherwise it is not augmented. The number of information input bits at the tth transition is given by $\lceil tm_k/n \rceil - \lceil (t-1)m_k/n \rceil$. For this variable state augmentation time-varying trellis, $\bar{i}_t = \underline{i}_t = t$ in the branch metrics in (12), (13), (14), and (15). The computational complexity of the variable state augmentation time varying trellis decoding is upper bounded by that of the CC multiplied by $2^{\tilde{m}-1}/\tilde{m} \cdot \tilde{i}$. If m_k is divisible by n then the CMT trellis is just m_k/n transitions in the CC trellis.

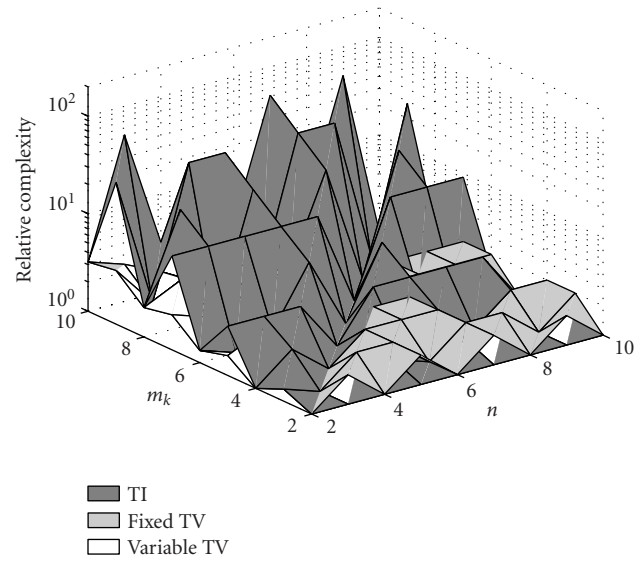

Figure 3: Complexity comparisons of time-invariant and time-varying trellises.

Time varying trellises were considered above based on the feedforward convolutional encoder. However, we can also develop time varying trellises with a recursive systematic convolutional code (RSCC). With RSCC, the information bit vector input can be dealt with because we know the primitive state transition in the code trellis. We can also treat the augmented state in RSCC.

The complexity relative to the CC complexity of time-invariant and two time-varying trellises are shown in Figure 3 for each n and m_k. "TI" denotes time-invariant trellis, "TV, fixed" time-varying trellis with fixed state augmentation and "TV, variable" time varying trellis with variable state augmentation.

4. PERFORMANCE ANALYSIS

4.1. Numerical approach

To find a tight numerical upper bound on the BER, the Laplace transform method based on Gauss-Chebyshev

quadrature rule is employed. We will focus on the analysis of CMT in this section, since the analysis of CT is simpler and conventional.

The optimal metric in (12) considers interference among multicode symbols $\mathbf{i}_i^k$, and correlation of $\bar{\mathbf{i}}_i^k$ and $\mathbf{n}_i^k$ for the same multicode symbols. If $\mathbf{i}_i^k$ and/or the correlation of $\bar{\mathbf{i}}_i^k$ and $\mathbf{n}_i^k$ are disregarded in the Viterbi decoder, it corresponds to employing one of the suboptimal metrics in (13), (14), and (15). The Viterbi decoder using the metric in (13) is $\mathbf{i}_i^k$-mismatched, and that using the metric in (14) is $(\bar{\mathbf{i}}_i^k + \mathbf{n}_i^k)$-mismatched. The metric in (15) is both $\mathbf{i}_i^k$- and $(\bar{\mathbf{i}}_i^k + \mathbf{n}_i^k)$-mismatched.

The evaluation of the PEP for a mismatched Viterbi decoder was analyzed in [9] but a true upper bound for BER using the transfer function method was not treated there. This problem was considered recently in [10] and the following derivation is based on the results in [10]. For the analysis, we employ the time-invariant trellis. We evaluate the PEP, $P(\mathbf{b}^{k,c} \to \mathbf{b}^{k,i})$ of choosing the incorrect code symbol sequence $\mathbf{b}^{k,i}$ when $\mathbf{b}^{k,c}$ was transmitted. Let M denote the length of the error event.

For the analysis of the Viterbi decoder employing the metrics in (12) and (13),

$$\begin{aligned} U_t^k &= \sum_{j=1}^{\tilde{I}} \Big(\Big(\mathbf{r}_{(t-1)\tilde{I}+j}^k - \mathbf{d}_{t,j}^{k,i}\Big)^T (\sigma^2\tilde{\mathbf{R}}^k + \bar{\mathbf{\Phi}}^k)^{-1} \Big(\mathbf{r}_{(t-1)\tilde{I}+j}^k - \mathbf{d}_{t,j}^{k,i}\Big) \\ &\qquad - \Big(\mathbf{r}_{(t-1)\tilde{I}+j}^k - \mathbf{d}_{t,j}^{k,c}\Big)^T (\sigma^2\tilde{\mathbf{R}}^k + \bar{\mathbf{\Phi}}^k)^{-1} \Big(\mathbf{r}_{(t-1)\tilde{I}+j}^k - \mathbf{d}_{t,j}^{k,c}\Big)\Big) \\ &= \sum_{j=1}^{\tilde{I}} U_{t,j}^k, \end{aligned} \tag{16}$$

and for the metrics in (14) and (15), let

$$\begin{aligned} U_t^k &= \sum_{j=1}^{\tilde{I}} \Big(\Big(\mathbf{r}_{(t-1)\tilde{I}+j}^k - \mathbf{d}_{t,j}^{k,i}\Big)^T \Big(\mathbf{r}_{(t-1)\tilde{I}+j}^k - \mathbf{d}_{t,j}^{k,i}\Big) \\ &\qquad - \Big(\mathbf{r}_{(t-1)\tilde{I}+j}^k - \mathbf{d}_{t,j}^{k,c}\Big)^T \Big(\mathbf{r}_{(t-1)\tilde{I}+j}^k - \mathbf{d}_{t,j}^{k,c}\Big)\Big) \\ &= \sum_{j=1}^{\tilde{I}} U_{t,j}^k, \end{aligned} \tag{17}$$

where for the $\mathbf{i}_i^k$-matched Viterbi decoder employing metrics in (12) and (14), $\mathbf{d}_{t,j}^{k,c} = \hat{\mathbf{R}}^k \mathbf{A}^k \mathbf{b}_{(t-1)\tilde{I}+j}^{k,c}$ and $\mathbf{d}_{t,j}^{k,i} = \hat{\mathbf{R}}^k \mathbf{A}^k \mathbf{b}_{(t-1)\tilde{I}+j}^{k,i}$, and for the $\mathbf{i}_i^k$-mismatched Viterbi decoder employing metrics in (13) and (15), $\mathbf{d}_{t,j}^{k,c} = (\hat{\mathbf{R}}^k \odot \mathbf{I}_k)\mathbf{A}^k \mathbf{b}_{(t-1)\tilde{I}+j}^{k,c}$ and $\mathbf{d}_{t,j}^{k,i} = (\hat{\mathbf{R}}^k \odot \mathbf{I}_k)\mathbf{A}^k \mathbf{b}_{(t-1)\tilde{I}+j}^{k,i}$.

Since $\hat{\mathbf{n}}_i^k$ and $\bar{\mathbf{i}}_i^k$ are i.i.d. in i, $U_t^{k,j}$ and $U_{t'}^{k,j'}$ are i.i.d. for $t \neq t'$ or $j \neq j'$. The Laplace transform of the pdf of $U^k = \sum_{t=1}^{M} \sum_{j=1}^{\tilde{I}} U_{t,j}^k$ for the metrics in (12) and (13) is

$$\begin{aligned} \Phi_{U^k}(\lambda) &= E\left\{ \exp\left(-\lambda \sum_{t=1}^{M} \sum_{j=1}^{\tilde{I}} U_{t,j}^k \right) \right\} \\ &= \prod_{t=1}^{M} \prod_{j=1}^{\tilde{I}} \exp\Big(-\lambda \Big[2\Big(\mathbf{b}_{(t-1)\tilde{I}+j}^{k,c}\Big)^T (\mathbf{A}^k)^T (\hat{\mathbf{R}}^k)^T \\ &\qquad \times (\sigma^2\tilde{\mathbf{R}}^k + \bar{\mathbf{\Phi}}^k)^{-1} [\mathbf{d}_{t,j}^{k,c} - \mathbf{d}_{t,j}^{k,i}] \\ &\qquad + \Big[(\mathbf{d}_t^{k,j,i})^T (\sigma^2\tilde{\mathbf{R}}^k + \bar{\mathbf{\Phi}}^k)^{-1} \mathbf{d}_{t,j}^{k,i} \\ &\qquad - (\mathbf{d}_{t,j}^{k,c})^T (\sigma^2\tilde{\mathbf{R}}^k + \bar{\mathbf{\Phi}}^k)^{-1} \mathbf{d}_{t,j}^{k,c} \Big] \Big] \\ &\qquad + 2\lambda^2 [\mathbf{d}_{t,j}^{k,c} - \mathbf{d}_{t,j}^{k,i}]^T (\sigma^2\tilde{\mathbf{R}}^k + \bar{\mathbf{\Phi}}^k)^{-1} \\ &\qquad \times [\mathbf{d}_{t,j}^{k,c} - \mathbf{d}_{t,j}^{k,i}] \Big), \end{aligned} \tag{18}$$

and for the metrics in (14) and (15) is

$$\begin{aligned} \Phi_{U^k}(\lambda) &= E\left\{ \exp\left(-\lambda \sum_{t=1}^{M} \sum_{j=1}^{\tilde{I}} U_{t,j}^k \right) \right\} \\ &= \prod_{t=1}^{M} \prod_{j=1}^{\tilde{I}} \exp\Big(-\lambda \Big[2\Big(\mathbf{b}_{(t-1)\tilde{I}+j}^{k,c}\Big)^T (\mathbf{A}^k)^T (\hat{\mathbf{R}}^k)^T \\ &\qquad \times [\mathbf{d}_{t,j}^{k,c} - \mathbf{d}_{t,j}^{k,i}] \\ &\qquad + \Big[(\mathbf{d}_{t,j}^{k,i})^T \mathbf{d}_{t,j}^{k,i} - (\mathbf{d}_{t,j}^{k,c})^T \mathbf{d}_{t,j}^{k,c} \Big] \Big] \\ &\qquad + 2\lambda^2 [\mathbf{d}_{t,j}^{k,c} - \mathbf{d}_{t,j}^{k,i}]^T (\sigma^2\tilde{\mathbf{R}}^k + \bar{\mathbf{\Phi}}^k) \\ &\qquad \times [\mathbf{d}_{t,j}^{k,c} - \mathbf{d}_{t,j}^{k,i}] \Big). \end{aligned} \tag{19}$$

The PEP is $P(\mathbf{b}^{k,c} \to \mathbf{b}^{k,i}) = P\,(U^k \leq 0)$ and is given by

$$\frac{1}{2\pi j} \int_{c-j\infty}^{c+j\infty} \Phi_{U^k}(\lambda) \frac{d\lambda}{\lambda} \tag{20}$$

for positive real constant c. By using the Gauss-Chebyshev rule, it can be obtained as [11]

$$\begin{aligned} &P(\mathbf{b}^{k,c} \longrightarrow \mathbf{b}^{k,i}) \\ &= \frac{1}{P} \sum_{p=1}^{P/2} \left(\Re\{\Phi_{U^k}(c + jc\tau_p)\} + \tau_p \Im\{\Phi_{U^k}(c + jc\tau_p)\} \right) + E_P, \end{aligned} \tag{21}$$

where $\tau_p = \tan((2p-1)\pi/(2P))$ and E_P is the error term.

By using (18), (19), and (21), we obtain the PEP in a product form and can find the union bound on BER by applying the transfer function method. Since uniformity does not hold for CMT, the transfer function bound is computed based on matrix branch labels instead of scalar branch labels. Let N_s be the number of states of the time-invariant trellis, which is 2^ν, equal to that of CC. Let $\mathbf{e}$ be the error code vector $\mathbf{c}^{k,c}(i,j) \oplus \mathbf{c}^{k,i}(i,j)$, where $\mathbf{c}^{k,c}$ and $\mathbf{c}^{k,i}$ are correct and incorrect output code bits corresponding to the transition from state j to state i, respectively. Let $\mathbf{c}^{k,l,c}(i,j) = [(\mathbf{c}^{k,c}(i,j))_{(l-1)m_k+1}, \ldots, (\mathbf{c}^{k,c}(i,j))_{lm_k}]^T$, $\mathbf{c}^{k,l,i}(i,j) = [(\mathbf{c}^{k,i}(i,j))_{(l-1)m_k+1}, \ldots, (\mathbf{c}^{k,i}(i,j))_{lm_k}]^T$ and $\mathbf{e}^{k,l} = [(\mathbf{e})_{(l-1)m_k+1}, \ldots, (\mathbf{e})_{lm_k}]^T$. For branch metrics (12) and (13)

let the $N_s \times N_s$ matrix $G_\lambda(\mathbf{e})$ be defined by

$$
\begin{aligned}
&(G_\lambda(\mathbf{e}))_{i+1,j+1} \\
&= 0, \quad \text{if no transition is possible,} \\
&= \frac{1}{2^{\bar{m}}} \prod_{l=1}^{\bar{i}} \exp\Big(-\lambda \Big[2(\mathbf{b}^{k,l,c}(i,j))^T (\mathbf{A}^k)^T (\hat{\mathbf{R}}^k)^T \\
&\qquad \times (\sigma^2 \tilde{\mathbf{R}}^k + \bar{\mathbf{\Phi}}^k)^{-1} [\mathbf{d}^{k,l,c}(i,j) - \mathbf{d}^{k,l,i}(i,j)] \\
&\qquad + \Big[(\mathbf{d}^{k,l,i}(i,j))^T (\sigma^2 \tilde{\mathbf{R}}^k + \bar{\mathbf{\Phi}}^k)^{-1} \\
&\qquad\quad \times \mathbf{d}^{k,l,i}(i,j) - (\mathbf{d}^{k,l,c}(i,j))^T \\
&\qquad\quad \times (\sigma^2 \tilde{\mathbf{R}}^k + \bar{\mathbf{\Phi}}^k)^{-1} \mathbf{d}^{k,l,c}(i,j) \Big] \Big] \\
&\qquad + 2\lambda^2 [\mathbf{d}^{k,l,c}(i,j) - \mathbf{d}^{k,l,i}(i,j)]^T \\
&\qquad \times (\sigma^2 \tilde{\mathbf{R}}^k + \bar{\mathbf{\Phi}}^k)^{-1} [\mathbf{d}^{k,l,c}(i,j) - \mathbf{d}^{k,l,i}(i,j)] \Big), \\
&\qquad\qquad \text{otherwise,}
\end{aligned}
\tag{22}
$$

where $\mathbf{b}^{k,l,c}(i,j) = 2\mathbf{c}^{k,l,c}(i,j) - \mathbf{1}_{m_k}$, $\mathbf{b}^{k,l,i}(i,j) = 2(\mathbf{c}^{k,l,i}(i,j) \oplus \mathbf{e}^{k,l}) - \mathbf{1}_{m_k}$, $\mathbf{d}^{k,l,c}(i,j) = \hat{\mathbf{R}}^k \mathbf{A}^k \mathbf{b}^{k,l,c}(i,j)$, and $\mathbf{d}_i^{k,l,i}(i,j) = \hat{\mathbf{R}}^k \mathbf{A}^k \mathbf{b}^{k,l,i}(i,j)$. $\mathbf{1}_n$ is $n \times 1$ vector whose elements are all ones. Similarly, for metrics (14) and (15), let $\mathrm{G}_\lambda(\mathbf{e})$ be

$$
\begin{aligned}
&(G_\lambda(\mathbf{e}))_{i+1,j+1} \\
&= 0, \quad \text{if no transition is possible,} \\
&= \frac{1}{2^{\bar{m}}} \prod_{l=1}^{\bar{i}} \exp\Big(-\lambda \Big[2(\mathbf{b}^{k,l,c}(i,j))^T (\mathbf{A}^k)^T (\hat{\mathbf{R}}^k)^T \\
&\qquad \times [\mathbf{d}^{k,l,c}(i,j) - \mathbf{d}^{k,l,i}(i,j)] \\
&\qquad + \Big[(\mathbf{d}^{k,l,i}(i,j))^T \mathbf{d}^{k,l,i}(i,j) \\
&\qquad\quad - (\mathbf{d}^{k,l,c}(i,j))^T \mathbf{d}^{k,l,c}(i,j) \Big] \Big] \\
&\qquad + 2\lambda^2 [\mathbf{d}^{k,l,c}(i,j) - \mathbf{d}^{k,l,i}(i,j)]^T \\
&\qquad \times (\sigma^2 \tilde{\mathbf{R}}^k + \bar{\mathbf{\Phi}}^k) [\mathbf{d}^{k,l,c}(i,j) - \mathbf{d}^{k,l,i}(i,j)] \Big), \\
&\qquad\qquad \text{otherwise,}
\end{aligned}
\tag{23}
$$

where $\mathbf{d}^{k,l,c}(i,j) = (\hat{\mathbf{R}}^k \mathbf{A}^k \odot \mathbf{I}_k)\mathbf{b}^{k,l,c}(i,j)$ and $\mathbf{d}^{k,l,i}(i,j) = (\hat{\mathbf{R}}^k \mathbf{A}^k \odot \mathbf{I}_k)\mathbf{b}^{k,l,i}(i,j)$.

Now define $\mathbf{G}_\lambda$ as

$$
\mathbf{G}_\lambda = \sum_{\mathbf{e}(0,0) \neq \mathbf{0}} \mathbf{G}_\lambda(\mathbf{e}) + \mathbf{C}_\lambda [\mathbf{I} - \mathbf{A}_\lambda]^{-1} \mathbf{B}_\lambda, \tag{24}
$$

where

$$
\begin{aligned}
\mathbf{C}_\lambda &= \left[\sum_{\mathbf{e}(0,1)} \mathbf{G}_\lambda(\mathbf{e}), \ldots, \sum_{\mathbf{e}(0,N_1)} \mathbf{G}_\lambda(\mathbf{e}) \right], \\
\mathbf{A}_\lambda &= \begin{bmatrix} \sum_{\mathbf{e}(1,1)} \mathbf{G}_\lambda(\mathbf{e}) & \cdots & \sum_{\mathbf{e}(1,N_1)} \mathbf{G}_\lambda(\mathbf{e}) \\ \sum_{\mathbf{e}(2,1)} \mathbf{G}_\lambda(\mathbf{e}) & \cdots & \sum_{\mathbf{e}(2,N_1)} \mathbf{G}_\lambda(\mathbf{e}) \\ \vdots & \ddots & \vdots \\ \sum_{\mathbf{e}(N_1,1)} \mathbf{G}_\lambda(\mathbf{e}) & \cdots & \sum_{\mathbf{e}(N_1,N_1)} \mathbf{G}_\lambda(\mathbf{e}) \end{bmatrix}, \\
\mathbf{B}_\lambda &= \left[\sum_{\mathbf{e}(1,0)} \mathbf{G}_\lambda(\mathbf{e}), \ldots, \sum_{\mathbf{e}(N_1,0)} \mathbf{G}_\lambda(\mathbf{e}) \right]^T,
\end{aligned}
\tag{25}
$$

$N_1 = N_s - 1$, and $\mathbf{e}(i,j)$ is the error code vector corresponding to the transition from error state j to error state i. The first error event probability (FEEP) is bounded by

$$
\mathrm{FEEP} \leq \frac{1}{P} \sum_{p=1}^{P/2} \left(\Re\{T_{c+jc\tau_p}\} + \tau_p \Im\{T_{c+jc\tau_p}\} \right) + E_P, \tag{26}
$$

where $T_\lambda = (1/N_s)\mathbf{1}_{N_s}^T G_\lambda \mathbf{1}_{N_s}$. The FEEP can also be evaluated by calculating residues of T_λ/λ. This requires the inverse of the symbolic matrix in (24) and as the state number of the trellis grows, it is infeasible to compute due to numerical problems. The Gauss-Chebyshev quadrature rule allows us to avoid numerical problems associated with the symbolic operation. When evaluating BER, the number of bits for each transition should be considered in the transfer function. In this case, we employ the first-order difference method in [12], avoiding the symbolic operation.

4.2. SIR-based approach

In Section 4.1, we presented a method to compute a tight upper bound for both CT and CMT numerically and the results are in good agreement with the simulation results (see Section 4). However, it does not explain qualitatively under what conditions CMT performs better than CT. Here, we present another method which can give some insight.

According to [6], the residual interference at the MMSE detector output is well approximated as Gaussian distributed and the probability of error of multicode j of user k at the MMSE detector output is given by $P_e^{k,j} = Q(\sqrt{\mathrm{SIR}_{k,j}})$, where

$$
\begin{aligned}
\mathrm{SIR}_{k,j} &= \frac{A_{k,j}^2 \left((\boldsymbol{\omega}_{k,j}^T \mathbf{R})_{\sum_{p=1}^{k-1} m_p + j} \right)^2}{\sigma^2 \tilde{\mathbf{R}}_{j,j}^k + \sum_{\substack{l=1, m=1 \\ l \neq k \text{ or } m \neq j}}^{K, m_l} A_{l,m}^2 \left((\boldsymbol{\omega}_{k,j}^T \hat{\mathbf{R}})_{\sum_{p=1}^{l-1} m_p + m} \right)^2} \\
&= \frac{A_{k,j}^2 ((\hat{\mathbf{R}})_{j,j}^k)^2}{[n_{k,j}^2[i]] + E[\tilde{i}_{k,j}^2[i]] + E[i_{k,j}^2[i]]}.
\end{aligned}
\tag{27}
$$

We use the decoding metrics in (11) for CT. In CMT, we assume that $E[(\mathbf{n}_i^k + \tilde{\mathbf{i}}_i^k + \mathbf{i}_i^k)(\mathbf{n}_i^k + \tilde{\mathbf{i}}_i^k + \mathbf{i}_i^k)^T] \approx (\sigma^2 \tilde{\mathbf{R}}^k + \bar{\mathbf{\Phi}}^k + \mathbf{\Phi}^k) \odot \mathbf{I}_k$, where the covariance matrix $\mathbf{\Phi}^k$ of $\mathbf{i}_i^k$ is

$$\mathbf{\Phi}^k = (\hat{\mathbf{R}}^k - (\hat{\mathbf{R}}^k \odot \mathbf{I}_k))\mathbf{A}^k(\mathbf{A}^k)^T(\hat{\mathbf{R}}^k - (\hat{\mathbf{R}}^k \odot \mathbf{I}_k))^T, \quad (28)$$

that is, all elements of $(\mathbf{n}_i^k + \bar{\mathbf{i}}_i^k + \mathbf{i}_i^k)$ are uncorrelated each other. Hence for CMT, we use the decoding metric

$$\mu_t^{k,5} = \sum_{i=\underline{i}_t}^{\bar{i}_t} (\mathbf{r}_i^k - (\hat{\mathbf{R}}^k \odot \mathbf{I}_k)\mathbf{A}^k\mathbf{b}_i^k)^T ((\sigma^2\tilde{\mathbf{R}}^k + \bar{\mathbf{\Phi}}^k + \mathbf{\Phi}^k) \odot \mathbf{I}_k)^{-1} \times (\mathbf{r}_i^k - (\hat{\mathbf{R}}^k \odot \mathbf{I}_k)\mathbf{A}^k\mathbf{b}_i^k), \quad (29)$$

and we see that decoding can be done in the code trellis with this metric.

We assume that a uniform interleaver with interleaver size N_i [13] is employed at the encoder output. The effect of the uniform interleaver is to make the SIR difference on each multicode channel disappear and hence uniformity holds for CMT. Thus, we can evaluate the union bound on BER by considering only the all-zero path as a reference path.

Consider an error event of length M and Hamming distance d from the all-zero path in the time-invariant trellis. If $N_i = M\tilde{m}n$, the uniform interleaver maps a given codeword with d "1" bits into $\binom{N_i}{d}$ distinct permutations with equal probability $1/\binom{N_i}{d}$. For each permutation index p, the set of indices of "1" bits in the trellis diagram is I_p. Then the SIR resulting from the comparison of two paths of Hamming distance d in CMT is given by

$$\sum_{p=1}^{\binom{N_i}{d}} \sum_{l\in I_p} \frac{1}{\binom{N_i}{d}} \mathrm{SIR}_{k,((l-1) \bmod m_k)+1} = \left(\sum_{j=1}^{m_k} \frac{1}{m_k} \mathrm{SIR}_{k,j}\right) d, \quad (30)$$

where l is the coded bit index in the trellis, since N_i is an integer multiple of m_k. Hence the PEP of the path of distance d in CMT is obtained as

$$P_{2,p}^k(d) = Q\left(\sqrt{\sum_{j=1}^{m_k} \frac{1}{m_k} \mathrm{SIR}_{k,j}\, d}\right). \quad (31)$$

In CT, the PEP of the path of distance d is given by

$$P_{1,p}^k(d) = \frac{1}{m_k} \sum_{j=1}^{m_k} Q\left(\sqrt{\mathrm{SIR}_{k,j}\, d}\right) \quad (32)$$

when it is averaged over multicodes.

Proposition 1. *$P_{2,p}^k(d) \le P_{1,p}^k(d)$ with equality if and only if all $\mathrm{SIR}_{k,j}$, $j = 1,\ldots,m_k$, are equal.*

Proof. $Q(\sqrt{\sum_{j=1}^{m_k}(1/m_k)\,\mathrm{SIR}_{k,j}\, d}) \le Q(\sum_{j=1}^{m_k}(1/m_k)\sqrt{\mathrm{SIR}_{k,j}\, d})$ for integer $m_k \ge 1$, because $Q(\cdot)$ is a monotonically decreasing function. Since $Q(x)$ is also a convex function for $x > 0$, $Q(\sum_{j=1}^{m_k}(1/m_k)\sqrt{\mathrm{SIR}_{k,j}\, d}) \le \sum_{j=1}^{m_k}(1/m_k)Q(\sqrt{\mathrm{SIR}_{k,j}\, d})$ by Jensen's inequality. The proposition follows. □

From the proposition, we can assert that CMT works better than CT. Furthermore, as $\mathrm{SIR}_{k,j}$, $j = 1,\ldots,m_k$, become more different, the advantage of CMT over CT gets larger. The PEP of CMT in this section provides optimistic performance since it is assumed that the elements of random vector $(\mathbf{n}_i^k + \bar{\mathbf{i}}_i^k + \mathbf{i}_i^k)$ are uncorrelated. However, the analysis gives some intuition where the multicode diversity comes from.

Next we comment on when the MMSE detector (8) actually provides different SIRs in (29). Note that $\mathbf{R}$ is a symmetric matrix with all diagonal terms equal to 1. As an extreme case, if all $A_{k,j}$ are equal and all off-diagonal terms of $\mathbf{R}$ are equal, all off-diagonal terms of $\mathbf{M}$ also become equal and equality of all $\mathrm{SIR}_{k,j}$ follows. Generally, the variation of crosscorrelations of two spreading codes increases when they are not synchronized. In ISI channels, when we consider the effective signature waveform of each user, the variation of crosscorrelations can be significant because the spreading codes are not synchronized in the effective signature waveform's crosscorrelation.

5. SIMULATION RESULTS

Computer simulations have been done for a BPSK system. Signature sequences with processing gain $N = 15$ were generated randomly and fixed.[1] The code rates of CCs were $1/n = 1/2$, 1/3, and 1/4, and the constraint length L is set to 5. The generator matrix is $[23\ \ 35]$, $[25\ \ 33\ \ 37]$, and $[25\ \ 27\ \ 33\ \ 37]$ for rates 1/2, 1/3, and 1/4 codes, respectively, and the decoding delay is $6L$. The cases where the desired user k has two, three, or four times faster information bit rates than others and all other users have the same data rates are considered. Thus, $m_k = 2, 3$, or 4, and $m_j = 1$ for $j \ne k$. The total number of users K is determined by $15 - (m_k - 1)$ and the total number of CDMA channels $C = \sum_{p=1}^{K} m_p$ is fixed at 15. The CDMA channel index $c_{k,j}$ for jth multicode of kth user is given by $c_{k,j} = \sum_{p=1}^{k-1} m_p + j$.

The case of matched m_k and n was simulated with $m_k = 2$, $n = 2$, and the results are shown in Figures 4 and 5. From the figures and Table 1, we see that when uncoded BERs of multicode channels at the MMSE detector output are similar, the performance improvement of CMT compared with CT is negligible; however, when the performances of multicode channels at MMSE detector output are very different, the performance gain of CMT over CT becomes significant. Also, the simulated BER of the MMSE detector is in good agreement with analytical BER. Simulation results of mismatched m_k and n are shown in Figures 6 and 7 and have similar behavior.

[1] The results for Gold codes in ISI channels are included in [14]. When random spreading codes which change for every bit period are employed, CT can exploit time diversity provided by them and the advantage of CMT disappears.

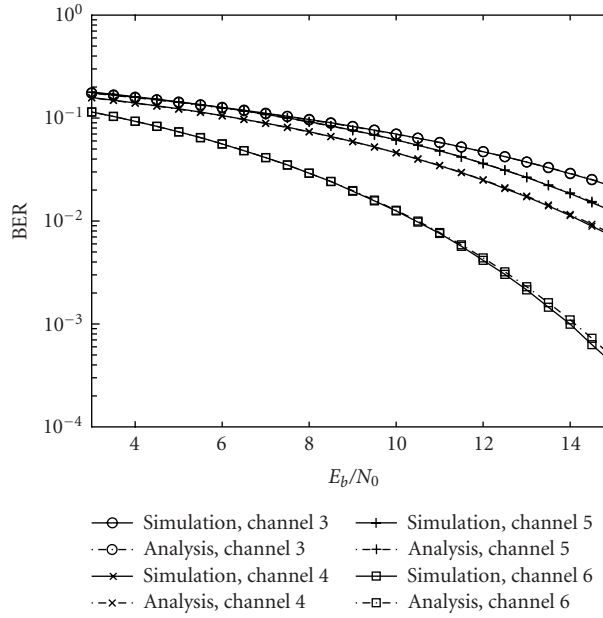

Figure 4: MMSE detector (uncoded) BER for CDMA channels 3, 4, 5, and 6, $C = 15$, $N = 15$.

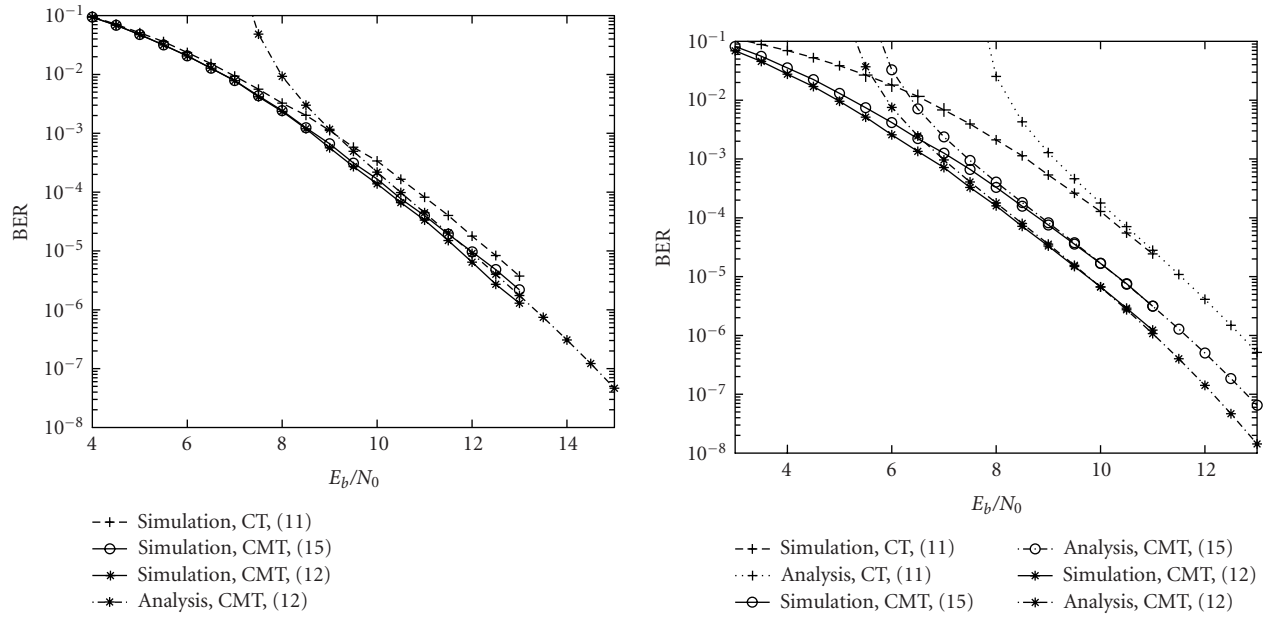

(a) (b)

Figure 5: (a) Coded BER, $K = 14$, $m_k = 2$, $n = 2$, $c_{k,1} = 3$, and $c_{k,2} = 4$. (b) Coded BER, $K = 14$, $m_k = 2$, and $n = 2$, $c_{k,1} = 5$, and $c_{k,2} = 6$.

Table 1: Comparison of CT and CMT when $n = 2$ and $m_k = 2$ (10 dB SNR).

	$c_{k,1} = 3$	$c_{k,2} = 4$	$c_{k,1} = 5$	$c_{k,2} = 6$
Uncoded BER	0.0702	0.0459	0.0610	0.0126
SIR	2.1874	2.8390	2.3873	4.9950
CT (11)	3.38×10^{-4}		1.28×10^{-4}	
CMT (15)	1.67×10^{-4}		1.68×10^{-5}	
CMT (14)	1.29×10^{-4}		1.23×10^{-5}	
CMT (13)	1.40×10^{-4}		7.59×10^{-6}	
CMT (12)	1.22×10^{-4}		6.72×10^{-6}	

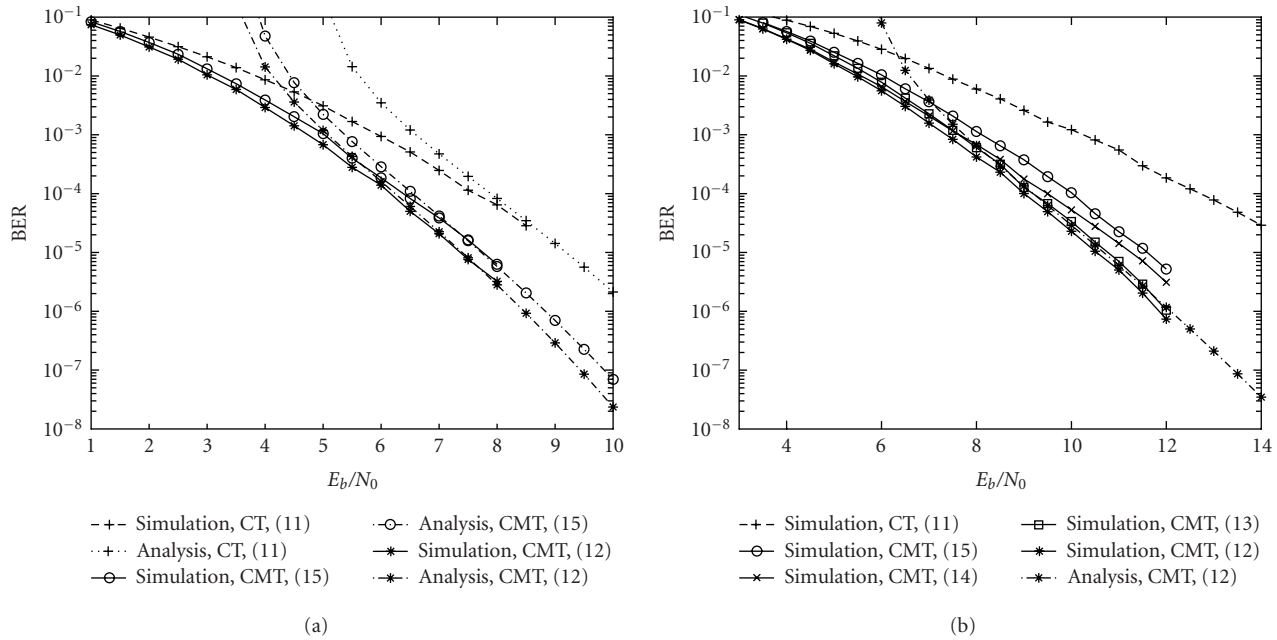

FIGURE 6: (a) Coded BER, $K = 14$, $m_k = 2$, $n = 4$, $c_{k,1} = 5$, and $c_{k,2} = 6$. (b) Coded BER, $K = 13$, $m_k = 3$, $n = 2$, $c_{k,1} = 5$, $c_{k,2} = 6$, $c_{k,3} = 7$.

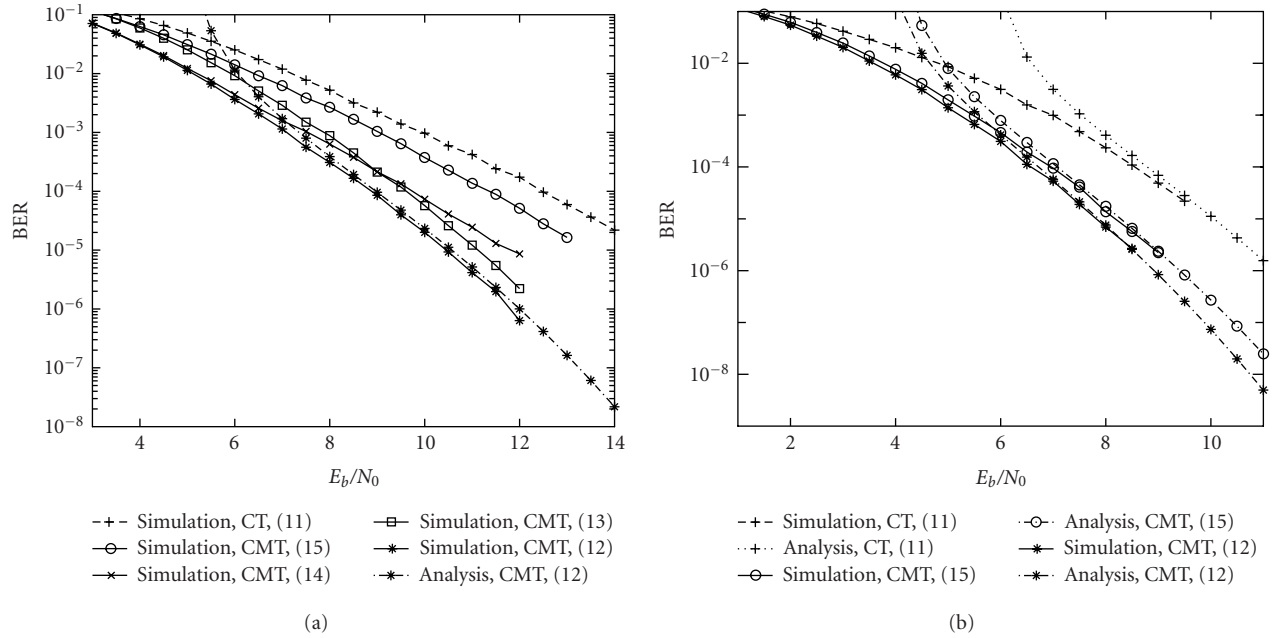

FIGURE 7: (a) Coded BER, $K = 12$, $m_k = 4$, $n = 2$, $c_{k,1} = 5$, $c_{k,2} = 6$, $c_{k,3} = 7$, and $c_{k,4} = 7$. (b) Coded BER, $K = 14$, $m_k = 2$, $n = 3$, $c_{k,1} = 5$, $c_{k,2} = 6$, and $c_{k,3} = 7$.

To examine the effect of crosscorrelation on the performance of CMT, the crosscorrelation

$$\mathbf{R} = \begin{pmatrix} 1.0 & 0.2 & 0.3 \\ 0.2 & 1.0 & \rho \\ 0.3 & \rho & 1.0 \end{pmatrix} \tag{33}$$

matrix was simulated with $0 \leq \rho \leq 0.95$ in the scenario where the desired user has two multicodes (channels 1 and 2) and another user has a single code (channel 3). Metrics in (11) and (15) are used for CT and CMT, respectively. In Figure 8, as ρ increases, the advantage of CMT over CT becomes more significant.

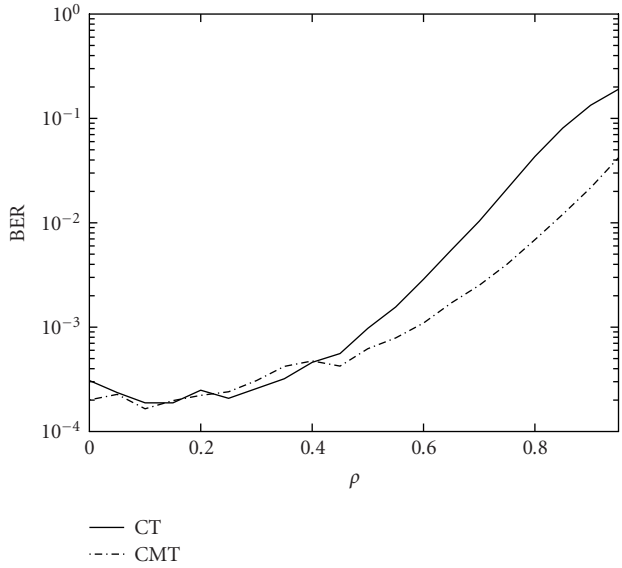

FIGURE 8: Coded BER for $0 \leq \rho \leq 0.95$, $K = 2$, $m_1 = 2$, $m_2 = 1$, $C = 3$, $c_{1,1} = 1$, $c_{1,2} = 2$ (3 dB SNR).

6. CONCLUSION

In this paper, we investigated two coding schemes combined with MMSE multiuser detection in multicode CDMA systems. Four metrics for CMT were considered along with different decoding trellises. Time invariant-trellises are employed for the analysis, and to reduce decoding complexity, time-varying trellises are used.

CMT generally provides better performance than CT with all four metrics. As the variation of SIRs among the multicodes increases at the MMSE detector output, the gain of CMT over CT becomes more significant. The Gauss-Chebyshev quadrature rule yielded a tight upper bound on BER using transfer function method. An SIR-based method provides insight into where the multicode diversity comes from.

ACKNOWLEDGMENT

This work is supported in part by NSF Grant CCR-1109580.

REFERENCES

[1] M. Zeng, A. Annamalai, and V. K. Bhargava, "Recent advances in cellular wireless communications," *IEEE Communications Magazine*, vol. 37, no. 9, pp. 128–138, 1999.

[2] C.-L. I, C. A. Webb III, H. C. Huang, S. T. Brink, S. Nanda, and R. D. Gitlin, "Is-95 enhancements for multimedia services," *Bell Labs Technical Journal*, vol. 1, no. 2, pp. 60–87, 1996.

[3] F. Adachi, M. Sawahashi, and H. Suda, "Wideband DS-CDMA for next generation mobile communication systems," *IEEE Communications Magazine*, vol. 36, no. 9, pp. 56–69, 1998.

[4] D. N. Rowitch and L. B. Milstein, "Convolutionally coded multicarrier DS-CDMA systems in a multipath fading channel. I. Performance analysis," *IEEE Trans. Communications*, vol. 47, no. 10, pp. 1570–1582, 1999.

[5] K. Ban, M. Katayama, W. E. Stark, T. Yamazato, and A. Ogawa, "Convolutionally coded DS/CDMA system using multi-antenna transmission," in *Proc. IEEE Global Telecommunications Conference*, vol. 1, pp. 92–96, Phoenix, Ariz, USA, November 1997.

[6] H. V. Poor and S. Verdu, "Probability of error in MMSE multiuser detection," *IEEE Transactions on Information Theory*, vol. 43, no. 3, pp. 858–871, 1997.

[7] J. R. Foerster and L. B. Milstein, "Coding for a coherent DS-CDMA system employing an MMSE receiver in a Rayleigh fading channel," *IEEE Trans. Communications*, vol. 48, no. 6, pp. 1012–1021, 2000.

[8] J. K. Cavers, J.-H. Kim, and P. Ho, "Exact calculation of the union bound on performance of trellis-coded modulation in fading channels," *IEEE Trans. Communications*, vol. 46, no. 5, pp. 576–579, 1998.

[9] O. E. Agazzi and N. Seshadri, "On the use of tentative decisions to cancel intersymbol interference and nonlinear distortion (with application to magnetic recording channels)," *IEEE Transactions on Information Theory*, vol. 43, no. 2, pp. 394–408, 1997.

[10] J.-H. Lim, *Combined predistortion and coded modulation in evolutionary digital satellite transmission systems*, Ph.D. dissertation, Purdue University, West Lafayette, Ind, USA, 2001.

[11] E. Biglieri, G. Caire, G. Taricco, and J. Ventura-Traveset, "Simple method for evaluating error probabilities," *Electronics Letters*, vol. 32, no. 3, pp. 191–192, 1996.

[12] A. J. Viterbi and J. K. Omura, *Principles of Digital Communication and Coding*, McGraw Hill, New York, NY, USA, 1979.

[13] S. Benedetto and G. Montorsi, "Unveiling turbo codes: some results on parallel concatenated coding schemes," *IEEE Transactions on Information Theory*, vol. 42, no. 2, pp. 409–428, 1996.

[14] J. Park, J.-H. Lim, and S. B. Gelfand, "Coding across multicodes and time in CDMA systems for dispersive channels," in *Proc. IEEE Wireless Communications and Networking Conference*, vol. 1, pp. 300–305, New Orleans, La, USA, March 2003.

Jeongsoon Park received his BSEE degree from Yonsei University, Korea in 1996 and his MSEE degree from Korea Advanced Institute of Science and Technology (KAIST), Korea in 1998, respectively. He is currently pursuing his Ph.D. degree in electrical engineering with Purdue University, Ind, where he is working on equalization and channel coding techniques for HDTV receivers and CDMA systems. His interests include equalization, channel coding, and iterative decoding.

Jong-Han Lim was born in Daegu, Korea, in 1967. He received the B.S. and M.S. degrees from Seoul National University in electrical engineering in 1990 and 1992, respectively. He received the Ph.D. degree from Purdue University, School of Electrical and Computer Engineering in 2001. From 1992 to 1994, he worked with Korea Telecom, Seoul, Korea, as a member of technical staff, where he participated in optical communication and remote maintenance system. From 1997 to 2001, he was a Research Assistant in the School of Electrical and Computer Engineering, Purdue University. Since 2001, he has been with Samsung Electronics. His current research interests include coded modulation, wireless communications, and digital communication system.

Saul B. Gelfand received the Ph.D. degree in electrical engineering and Computer Science from MIT in 1987. Previously he was with Scientific Systems, Inc., Cambridge, MA, and Bolt Beranek and Newman Inc., Cambridge, MA. In these positions he worked on multitarget detection and tracking problems in sonar signal processing. Since 1987 he has been with the School of Electrical and Computer Engineering, Purdue University, West Lafayette, Ind, where he is a Professor. His major contributions lie in the formulation and analysis of recursive algorithms for detection, estimation, filtering, and optimization of stochastic systems, with primary application to digital communications and biomedical signal processing. Professor Gelfand has previously served as Editor for Equalization for the IEEE Transactions on Communications, and Chair of the Communications Theory Symposium at the 2000 IEEE International Conference on Communication.